ELSEVIER

Removal of azo-dye Acid Red B (ARB) by adsorption and catalytic combustion using magnetic $CuFe_2O_4$ powder

Rongcheng Wu, Jiuhui Qu*, Hong He, Yunbo Yu

Research Center for Eco-Environmental Sciences, Chinese Academy of Sciences, Beijing 100085, China

Abstract

The effectiveness of magnetic $CuFe_2O_4$ powder as adsorbent/catalyst for the removal of azo-dye Acid Red B (ARB) from water by adsorption and subsequent catalytic combustion was studied. Magnetic $CuFe_2O_4$ powder showed excellent adsorption properties towards ARB at pH < 5.5, and it could be conveniently recovered by magnetic separation technology after adsorption. The combustion decomposition of ARB in the presence or absence of $CuFe_2O_4$ was studied by a system for thermal degradation studies (STDS) and in situ FTIR. The results indicated that different reactive pathways existed for the combustion under different conditions. In the presence of $CuFe_2O_4$, the temperature needed for oxidation reaction and for combustion was 150 and 300 °C, respectively. The reaction products were observed to be SO_2, CO_2, H_2O, and nitrate. There was neither volatile organic compound (VOCs) emitted to atmosphere during reaction nor organic matter deposited on the surface of $CuFe_2O_4$ after the combustion. Comparatively, in the absence of $CuFe_2O_4$, the oxidation and combustion of ARB required a higher temperature (300 and 500 °C, respectively) and produced a lot of toxic organic compounds emitted to atmosphere besides SO_2, CO_2 and H_2O during the reaction. In addition, sulfate was generated instead of nitrate. The experiments of adsorption–combustion cycles demonstrated that there was no evident change in adsorption properties and catalytic activity of magnetic $CuFe_2O_4$ powder after seven cycles.
© 2003 Elsevier B.V. All rights reserved.

1. Introduction

The complete mineralization of organic pollutants is the safest method to the environment, and some technologies, such as biotechnology and chemical oxidations, have been studied for or applied to the treatment of organic pollutants in water, atmosphere or soil [1,2]. But some of the contaminants such as aromatic halide or nitro aromatic substance and dyes have adequate resistance to oxidation by bio-degradation and conventional chemical oxidation. In view of the growing concern of environmental issues, alternative techniques must be found to meet the problem. Adsorption process and catalytic oxidation technologies are promising methods for the removal of various contaminants and have been studied for the removal of organic refractory pollutants from water [3,4].

Adsorption process is one of the effective methods with the advantages of high treatment efficiency and no harmful by-product to treated water [5]. But adsorption process just transfers pollutants from one phase to another rather than eliminating them from the environment. When the adsorbents are used to adsorb toxic compounds or to decontaminate effluents, they become hazardous wastes that should be treated or disposed properly.

Catalytic oxidation has been extensively studied for the destruction of refractory and hazardous pollutants found in groundwater, surface water, and industrial wastewater. Currently, these oxidation technologies are usually used directly in raw water matrix for decomposing organic compounds [6,7]. However, these processes often have the disadvantages of the too large volumes of raw water to be treated in the oxidation system and, in some cases, incomplete mineralization of some contaminants and probably with some more toxic substances produced leading to the secondary pollution of the treated water or atmosphere [7]. In addition, it seems that the lower the concentration of contaminants is, the higher the cost for the mineralization of a defined amount of organic compounds tends to be.

So it appears attractive to combine adsorption with catalytic oxidation in a water treatment system, in which the

contaminants are removed at first from a large volume of effluent by adsorption and pre-concentrated on adsorbent/catalyst material; and then separated from water; at last, mineralized by catalytic oxidation on the adsorbent/catalyst material, and the adsorbent/catalyst is regenerated at the same time. In such a process, the adsorption and oxidation operation is performed in different units, so the quality of treated water is only affected by the adsorption efficiency.

To achieve higher water treatment efficiency, the properties of adsorbent/catalyst are very important, including significant organic pollutant adsorption from solution and high catalytic activity for oxidation. At present, few of materials possess the property combining sufficient adsorption efficiency and excellent catalytic activity. There is a growing interest in inexpensive high surface area materials, especially metal oxides, and in their unique applications including adsorption and chemical catalysis [8,9]. It is known that the smaller the particles of adsorbent or catalyst are, the better its properties are, but the more difficult the recovery is. Powder iron oxides have relatively high surface area and catalytic activity. Many researchers have used the iron oxides to remove heavy metals and organic pollutants from tap or waste water [10,11]. Herrera et al. have studied the effectiveness of hematite fine particles as adsorbent/catalyst for adsorbing and catalytic combusting azo-dye Orange II and showed good results for the adsorption of hematite towards Orange II at about pH 3. But the solid/liquid separation was difficult and there were some harmful VOCs by-products formed during the combustion [12].

Magnetic separation is considered as a high speed and effective technique for separating magnetic particles. It has been used for many applications in biochemistry, microbiology, cell biology, analytical chemistry, mining ores, and environmental technology [13,14]. Thus, if the powder adsorbent/catalyst are magnetic, it could be recovered conveniently by magnetic separation technology.

It is known that copper ferrite is magnetic material. In this study, we evaluated the effectiveness of magnetic ferrite $CuFe_2O_4$ powder as an adsorbent/catalyst material for the removal of azo-dye Acid Red B (ARB), as a model organic pollutant, by adsorption–catalytic combustion. We focused on: firstly, the adsorption properties of magnetic $CuFe_2O_4$ powder towards ARB; secondly, the catalytic activity for adsorbed ARB combustion and the analyses of products formed during the reaction; and thirdly, the reusability of magnetic $CuFe_2O_4$ powder as an adsorbent/catalyst.

2. Experimental

2.1. Materials

$CuFe_2O_4$ was prepared by co-precipitation method. 0.01 mol $Cu(NO_3)_2 \cdot 3H_2O$ and 0.02 mol $Fe(NO_3)_3 \cdot 9H_2O$ was dissolved in 100 ml of distilled water. Under vigorous magnetic-stirring, slowly raised the pH by adding 10%

NaOH solution to around 10 and continued stirring for 30 min, and then stopped stirring. The suspension was heated to 95–100 °C for 2 h. After cooling, the prepared magnetic adsorbent was repeatedly washed with distilled water. By magnetic separation, the solid was separated from water and dried at 50 °C for 5 h and at 110 °C for 3 h. The dry material was crushed and then calcinated at 300 °C for 1 h.

ARB was purchased from Beijing Chemicals Co. (Beijing, China) and used without further purification. Its structure is:
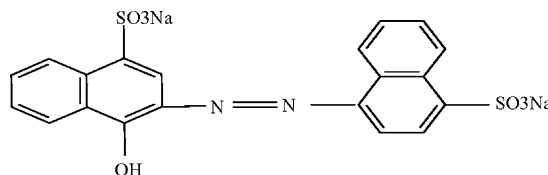
Deionized water was used throughout this study.

2.2. Methods

The crystalline structure of $CuFe_2O_4$ was determined using the X-ray powder diffraction method with a Rigaku III/B MAX diffractometer using Ni-filtered Cu Kα radiation.

Specific saturation magnetization (σ_s) which is a measure of particle's magnetism was determined using a VSM model 155 magnetic meter.

Scanning electron microscopy/energy dispersive X-ray (SEM/EDAX) was carried out by means of Hitachi S-3500N Scanning Electron Microscope with an EDAX KEVEX Level 4.

BET surface area, pore diameter, and pore volume were determined by an ASAP2000 surface analyzer (Micromeritics Co., USA) and N_2 as the adsorbate. Particle size of the adsorbent was determined by a Mastersizer 2000 (Malvern Co.).

Adsorption studies were carried out in glass vessels with agitation provided by a shaker. The temperature was controlled at 25 °C by air bath. The pH was adjusted by addition of HCl or NaOH. The suspension containing 0.100 g $CuFe_2O_4$ adsorbent and varying amount of ARB was shaken on an orbit shaker at 140 rpm. Samples were taken at different time intervals. The concentration of ARB was determined by spectrophotometer (U-3010, Hitachi Co.) at 516 nm or by TOC analyzer (Phoenix 8000, Tekmar Dohrmann Co., USA) after 0.45 μm membrane filtration.

For the adsorption rate and the effect of pH on adsorption experiments, 50 ml ARB solution (100 mg/l) was used. Adsorption isotherms were conducted using the completely mixed batch reactor bottle-point method, and the solution pH was at 4.8.

The powder $CuFe_2O_4$ adsorbent was recovered by magnetic separation method with a permanent magnet of 40 mm diameter and 10 mm thickness, made with Nd–Fe–B (2300 G).

Thermal degradation tests were carried out with the following processes: After adsorption and magnetic separa-

tion, the collected powder $CuFe_2O_4$ adsorbent containing adsorbed ARB was dried at 50 °C, and then placed into a quartz reactor. The air was let in at a flow of 30 ml/min, and the quartz reactor temperature raised at 30 °C/min and kept for 10 min at each specified temperature. The outlet gas with reaction products was first swept into a collector kept at 40 °C for collecting reaction products which can be condensed below 40 °C. And then, from the collector, the gas was subsequently transferred into a high resolution mass spectrometer through a pipeline kept at 100 °C for the analysis of low boiling point products. The MS was setup by scan mode at lowmass = 45 and highmass = 350.

The reaction products collected at 40 °C were dissolved in CH_2Cl_2 and analyzed by a GC–MS instrument (GC: HP6890; MS: HP5973) equipped with a HP-5MS column (60 m × 0.32 mm, 0.25 μm film thickness). The oven temperature was held at 40 °C for 2 min and then increased at a rate of 10 °C/min up to 280 °C and held for 5 min. By this system, all the VOCs formed during the catalytic combustion were determined qualitatively once the reaction started.

Diffuse reflectance (DRIFT) spectra of the azo-dye ARB and adsorbed ARB on $CuFe_2O_4$ were determined by a Nicolet 670 FTIR spectrophotometer equipped with a controlled-temperature and environment diffuse reflectance in situ chamber and a liquid nitrogen-cooled HgCdTe detector.

After catalytic combustion, the regenerated $CuFe_2O_4$ was recovered and was followed by washing with 10 ml NaOH solution of pH 8–9 for further tests.

3. Results and discussion

3.1. Characteristics of $CuFe_2O_4$

The XRD analysis indicated the spinel structure of $CuFe_2O_4$, and surface morphology analysis by SEM showed the agglomeration of many microfine particles with diameter of about 100 nm, which led to a rough surface and the presence of pores structure. The main characteristics of prepared $CuFe_2O_4$ are given in Table 1. It can be seen that $CuFe_2O_4$ powder has a surface area of 88.6 m²/g, a mesopore structure with average pore diameter 70.2 Å and a fine particle size of 11.7 μm. All these characteristics are in favor of adsorption. The specific saturation magnetization σ_s is 22.8 emu/g. And in a batch experiment, 0.5 g of the magnetic powder $CuFe_2O_4$ adsorbent in 100 ml H_2O was used for recovery test and a recovery ratio of above 98% was achieved with a permanent magnet (2300 G). A
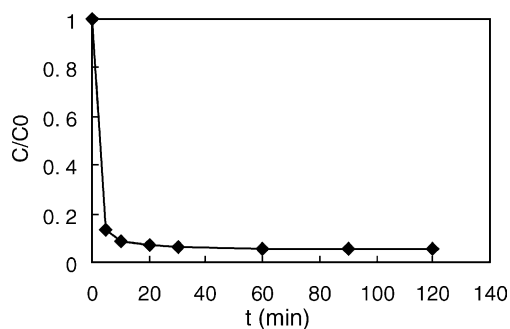

Fig. 1. Adsorption rate of ARB on $CuFe_2O_4$. (50 ml ARB solution, initial concentration 100 mg/l, pH 4.8; 0.100 g $CuFe_2O_4$.)

higher recovery ratio could be attained if the magnetic field strength of permanent magnet is higher and much more of the magnetic adsorbent $CuFe_2O_4$ is used. Therefore, the magnetic adsorbent $CuFe_2O_4$ powder can be recovered efficiently by magnetic separation technology after adsorption or regeneration.

3.2. Adsorption of ARB onto $CuFe_2O_4$

3.2.1. Adsorption rate

The effect of contact time on the removal of ARB by $CuFe_2O_4$ is illustrated in Fig. 1. As expected, the adsorption rate was very fast, and the equilibrium adsorption was almost achieved within 30 min. This may be due to the fine particles of $CuFe_2O_4$ powder of average size 11.7 μm and of mesopore structure as presented in Table 1. The smaller particle size was favorable for both the diffusion of dye molecules onto the active site of adsorbent and the complexation between the dye molecules and adsorbent. As a result, a higher adsorption efficiency was realized in a shorter adsorbing time.

3.2.2. Effect of pH on ARB removal

The effect of solution pH on adsorption varies significantly with different adsorbent or adsorbate. Fig. 2 shows the removal of ARB by $CuFe_2O_4$ at various pH. 50 ml ARB solution at the initial dye concentration of 100 mg/l was used. It indicates that the removal of ARB was strongly dependent on pH. Acidic condition was favorable, especially at pH < 5.5. In this condition, the removal of ARB above 95% was achieved. So adsorption of ARB by $CuFe_2O_4$ should be performed at pH < 5.5.

3.2.3. Adsorption isotherm

Adsorption capacity at different aqueous equilibrium concentration can be illustrated by the adsorption isotherm.

Table 1
Characteristics of magnetic $CuFe_2O_4$ powder

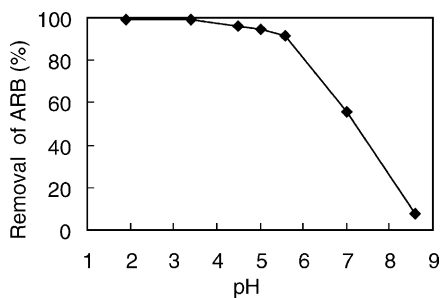| Particle size (μm)	Specific saturation magnetization (emu/g)	Surface area (m²/g)	Average pore diameter (Å)	Average pore volume (cm³/g)
11.7	22.8	88.6	70.2	0.14

Fig. 2. Effect of pH on ARB removal. (50 ml ARB solution, initial concentration 100 mg/l, pH 4.8; 0.100 g CuFe$_2$O$_4$.)

Fig. 3 shows the adsorption isotherm of ARB on CuFe$_2$O$_4$ at pH 4.8 and 20 °C. It is noted that the curve has a high slope in the initial portion and then levels off. This indicates that CuFe$_2$O$_4$ adsorbent has high adsorption density even at low equilibrium dye concentrations c_e and it also indicates that CuFe$_2$O$_4$ has a high affinity for ARB molecules, and this is favorable for removing dye from water to a lower concentration.

The adsorption data in Fig. 3 were fitted to Langmuir adsorption model very well with correlation coefficient $R^2 = 0.998$. The calculated maximum adsorption capacity q_m of ARB on CuFe$_2$O$_4$ at pH 4.8 is 86.8 mg/g.

Langmuir equation:

$$q_e = \frac{q_m k c_e}{1 + k c_e}$$

where q_e (mg dye/g adsorbent) is the amount of dye adsorbed per gram of adsorbent at equilibrium; q_m (mg dye/g adsorbent) is the maximum adsorption capacity; k (l/mg) is the equilibrium adsorption constant; and c_e (mg/l) is the equilibrium concentration of dye in solution.

The adsorption test indicated that CuFe$_2$O$_4$ was an excellent adsorbent for ARB adsorption at pH < 5.5.

3.2.4. FTIR spectra for ARB adsorption

The FTIR spectra of ARB, adsorbed ARB on CuFe$_2$O$_4$ and initial CuFe$_2$O$_4$ is shown in Fig. 4. The peaks at 1603 and 1501 cm^{-1} are assigned to aromatic C=C stretching vibration [15], while the weak peak at 1463 cm^{-1} is correspond to –N=N– bond stretching vibration, and 1207, 1436 cm^{-1} are assigned to –C–O– bond stretching vibration
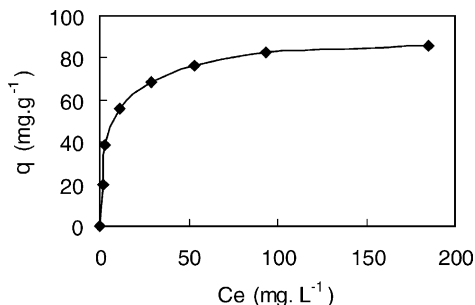

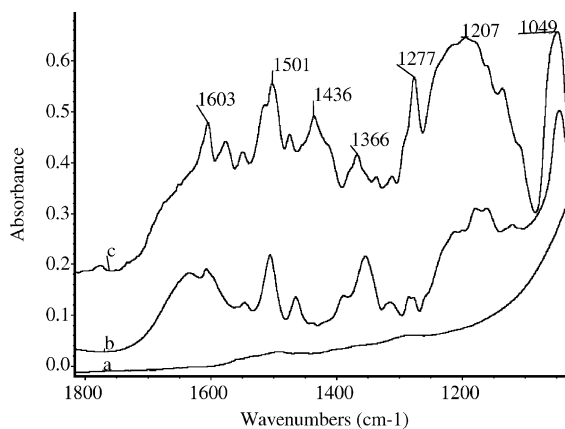Fig. 3. Adsorption isotherm ARB on CuFe$_2$O$_4$ at pH 4.8.

Fig. 4. FTIR spectra for ARB adsorption on CuFe$_2$O$_4$: (a) CuFe$_2$O$_4$, (b) ARB adsorbed on CuFe$_2$O$_4$, and (c) ARB.

and –OH deformation, respectively. The –SO$_3$$^-$ asymmetric vibrations is shown at 1277 cm^{-1} [16] and its symmetric stretching vibration overlaps with that of –C–O– bond at about 1200 cm^{-1}. It can be seen that peaks of adsorbed ARB on CuFe$_2$O$_4$ were similar to those of ARB except for the peaks at 1436 cm^{-1} (–OH) and 1277 cm^{-1} (–SO$_3$$^-$) that almost disappeared after adsorption, and the peak at 1200 cm^{-1} also changed obviously. This suggests the participation of both –C–OH and –SO$_3$$^-$ groups in bond formation with the adsorbent surface [17] and confirms the chemisorption of ARB on CuFe$_2$O$_4$.

3.3. Catalytic combustion of ARB on CuFe$_2$O$_4$

3.3.1. Thermal degradation studies by system for thermal degradation studies (STDS)

In the test, 50 mg ARB (by itself or adsorbed on CuFe$_2$O$_4$) was placed into the quartz reactor. The air was let in at a flow of 30 ml/min, the quartz reactor temperature was raised to 30 °C/min and kept for 10 min at each specified temperature. The outlet gas with reaction products was first swept into a collector kept at 40 °C for collecting high boiling point reaction products, and then the outlet gas was subsequently transferred into a high resolution mass spectrometer through a pipeline kept at 100 °C for the analysis of low boiling point products. The MS was setup by scan mode at lowmass = 45 and highmass = 350. The high boiling point reaction products collected at 40 °C were dissolved in CH$_2$Cl$_2$ and analyzed by GC–MS. By this system, all the volatile organic compounds formed during the catalytic combustion were determined qualitatively once the reaction occurred.

Fig. 5 shows the ions abundance of reaction products at various temperature. It is indicated in Fig. 5 that the lowest temperature required for oxidation reaction in the presence or absence of CuFe$_2$O$_4$ was very different. In the presence of CuFe$_2$O$_4$, the oxidation reaction started at about 155 °C, which was 180 °C lower than that of the reaction in the absence of CuFe$_2$O$_4$. By ion search, only two peaks at m/z 48 and 64, corresponding to SO$_2$, appeared in the mass
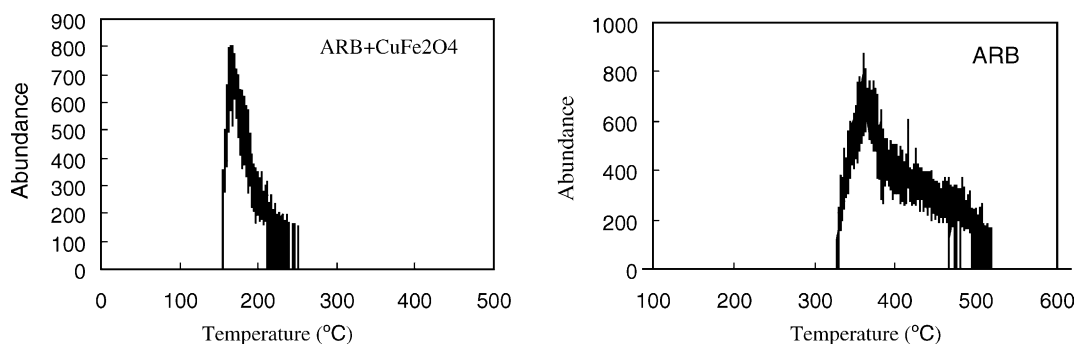
Fig. 5. Ions abundance for ARB combustion at various temperatures in the presence or absence of $CuFe_2O_4$.

spectra for ARB/$CuFe_2O_4$ reaction. While in the absence of $CuFe_2O_4$, more peaks appeared in the mass spectra including the peaks at m/z 45 (CH_3NO or HCO–NH_2), m/z 45 and 60 (CH_3NH–$NHCH_3$), m/z 48 and 64 (SO_2). This indicated that $CuFe_2O_4$ has excellent catalytic activity for ARB combustion, allowing a lower reaction temperature and no low boiling-point organic compound produced. Comparatively, a higher reaction temperature was needed in the absence of $CuFe_2O_4$ and much more by-products were generated.

The reaction products collected at $40\,^{\circ}C$ for ARB combustion at different temperatures in the presence or absence of $CuFe_2O_4$ were also analyzed by GC–MS. The most important by-products detected are reported in Table 2. It is noted in Table 2 that at all the temperatures used, no by-product was observed for the combustion of ARB in the presence of $CuFe_2O_4$. These results proved the total mineralization of ARB to CO_2. In comparison, at the same temperature but in the absence of $CuFe_2O_4$, the thermal degradation of ARB led to a lot of organic by-products, such as: phenol, naphthalene, naphthol, aminonaphthalene, nitrile, phthalimide, $1,1'$-dinaphthyl ether, and polycyclic aromatic hydrocarbons (PAHs). At higher temperatures, the number of by-products generally increased. This was in consistent with the results of oxidation of another azo-dye Orange II studied by Herrera et al. [12]. But in Herrera's study, there were also some harmful VOCs by-products, such as benzene, 2-naphthol, and nitrile, formed and emitted during the combustion in the presence of hematite at the temperature 250–$600\,^{\circ}C$. Therefore, the catalytic activity of $CuFe_2O_4$ is higher than that of hematite.

The carbon balance during the combustion of adsorbed dye was also studied. In the test, a solution of $0.1\,mol/l$ NaOH was used to collect the gas produced during the reaction. After reaction, inorganic carbon (IC) and total organic carbon (TOC) of the solution were determined by IC/TOC analyzer. A blank experiment on the air collection was carried out at the same time to eliminate the influence of atmospheric CO_2 on IC analysis. It was found that TOC of the solution was negligible. IC analysis indicated that nearly 100% of the initial C-content of the dye adsorbed on the $CuFe_2O_4$ was degraded to CO_2. Only trace amounts of carbon were found on the $CuFe_2O_4$ surface after combustion

and it might come from organic contaminants or adsorbed CO_2.

The STDS experiment indicated the excellent catalytic activity of $CuFe_2O_4$ for adsorbed ARB combustion in air atmosphere. In the presence of $CuFe_2O_4$, a lower temperature needed for reaction was allowed, and there were no VOCs emitted to environment during the combustion. In comparison, without $CuFe_2O_4$, the temperature needed for oxidation reaction was higher, and there were lots of toxic VOCs emitted to environment during the combustion.

3.3.2. In situ FTIR studies for ARB and ARB/CuFe2O4 combustion reaction

As mentioned above, the combustion of ARB in the presence or absence of $CuFe_2O_4$ showed marked difference both in the temperature needed for reaction and the reaction products. In order to obtain insights into the reaction process, combustion of ARB in the presence or absence of $CuFe_2O_4$ was studied by means of in situ DRIFT spectroscopy. In the test, 10 mg ARB (by itself diluted by KBr or adsorbed on $CuFe_2O_4$) were placed into the in situ reactor, and the air was let in at a flow of 30 ml/min. The infrared spectra of the combustion at different temperatures are shown in Figs. 6 and 7 for ARB and ARB/$CuFe_2O_4$, respectively.

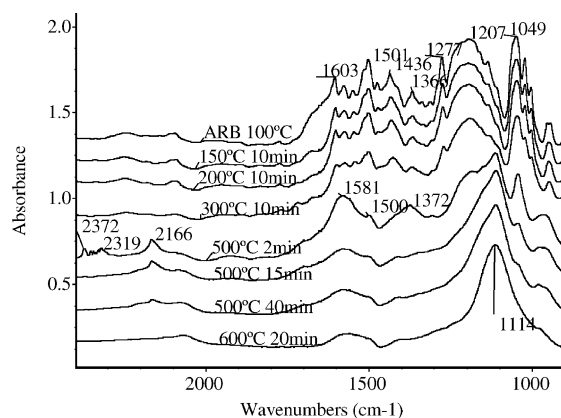In the absence of $CuFe_2O_4$, ARB was stable at the temperature below $300\,^{\circ}C$ (Fig. 6). At $300\,^{\circ}C$, the peaks
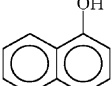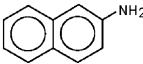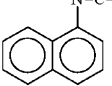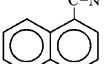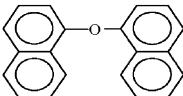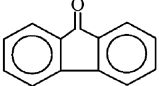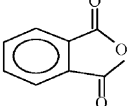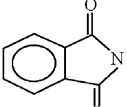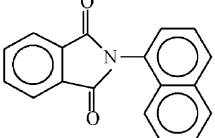
Fig. 6. FTIR spectra for ARB combustion in the absence of $CuFe_2O_4$ at different temperatures.

Table 2
By-product identification during ARB combustion at different temperature in the presence or absence of $CuFe_2O_4$

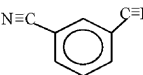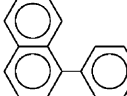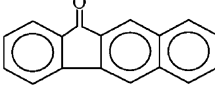| No.	Compound	ARB + $CuFe_2O_4$ (300 °C)	ARB (300 °C)	ARB (400 °C)	ARB '(500 °C)	ARB (500 °C)
1		No	Yes	Yes	Yes	Yes
2		No	Yes	Yes	Yes	No
3		No	Yes	No	No	Yes
4		No	Yes	Yes	Yes	Yes
5		No	Yes	Yes	Yes	Yes
6		No	No	Yes	Yes	No
7		No	No	Yes	Yes	Yes
8		No	No	No	Yes	Yes
9		No	No	No	No	Yes
10		No	No	No	No	Yes
11		No	No	No	No	Yes
12		No	No	No	No	Yes
13		No	No	No	No	Yes
14		No	No	No	No	Yes

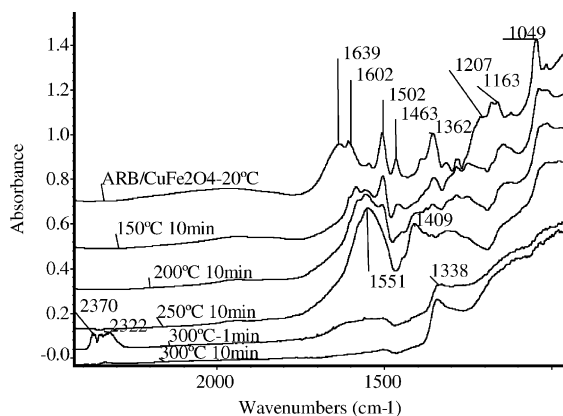Fig. 7. FTIR spectra for ARB/CuFe$_2$O$_4$ combustion at different temperatures.

of ARB were similar to those of ARB at the temperature below 300 °C except that the peak at 1277 cm^{-1} (–SO$_3^-$) decreased and the weak peak at 1463 cm^{-1} (–N=N–) almost disappeared after 10 min. This suggests the reaction of N=N– and –SO$_3^-$ at 300 °C, and this initial reaction temperature was in consistent with the results by STDS studies described previously. At 500 °C, the spectra changed drastically after heating 2 min. The asymmetric vibration O–S(O$_2$) at 1277 cm^{-1} disappeared, while the stretching vibration C=C and C–O at 1500 and 1207 cm^{-1} also decreased, respectively. Simultaneously, some new peaks appeared at 1114 cm^{-1} (SO$_4^{2-}$), 1372 cm^{-1} (–NO$_2$), 1581 cm^{-1} (–NO), 2166 cm^{-1} (–C≡N or N=C=O). CO$_2$ peaks between 2319 and 2372 cm^{-1} also appeared. All these indicated the fast oxidation of ARB with the production of CO$_2$, sulfate and some organic by-products. After 40 min, the peaks at 1372 cm^{-1} (–NO$_2$) and 1207 cm^{-1} (C–O) disappeared, the peak at 2166 cm^{-1} (–C≡N or –N=C=O) and the peaks between 1500 and 1600 cm^{-1} (C=C) decreased, but not disappeared completely. Even at 600 °C, and reacted for 20 min, the peaks between 1500 and 1600 cm^{-1} still remained. These results indicated that, at 500 °C, all groups of ARB molecules were oxidized, but the oxidation was not complete even at the temperature as high as 600 °C. The residues included some organic compounds and sulfate, but no visible amount of nitrate was generated.

Fig. 7 shows the combustion reaction of adsorbed ARB in the presence of CuFe$_2$O$_4$. It can be seen that at 150 °C, the spectra already changed evidently: the peaks between 1100 and 1250 cm^{-1} (–SO$_3^-$ and –C–O) decreased, which means the reaction of ARB on CuFe$_2$O$_4$ at 150 °C. This is also consistent with the results by STDS studies. At 200 °C, the changes in spectra were more drastic: The peaks between 1100 and 1250 cm^{-1} (–SO$_3^-$ and –C–O) and 1463 cm^{-1} (–N=N–) were very weak, while a new peak at 1551 cm^{-1} (–NO$_2$) appeared. This indicated that the oxidation of –N=N– to nitro-compounds and the further oxidation of –SO$_3^-$ and –C–OH had taken place. At 250 °C, the peaks between 1100 and 1250 cm^{-1} (–SO$_3^-$ and –C–O) and 1463 cm^{-1} (–N=N–) almost disappeared and the peak at 1551 cm^{-1} (–NO$_2$) increased rapidly. At 300 °C, the peaks between 1500 and 1650 cm^{-1} (C=C, and –NO$_2$) decreased drastically, and the peaks at 1338 cm^{-1} (NO$_3^-$), 2321–2370 cm^{-1} (CO$_2$) appeared rapidly at the same time, which confirmed that the fast oxidation of aryl and –NO$_2$ to CO$_2$ and nitrate had taken place, respectively. After 10 min reaction, only the peak at 1338 cm^{-1} (NO$_3^-$) left was obvious, while the peak at 1114 cm^{-1} (SO$_4^{2-}$) was very weak. It is indicated in Fig. 7 that the adsorbed ARB was completely oxidized by catalytic combustion in the presence of CuFe$_2$O$_4$ and no organic compound residue left after combustion. Nitrate was the main residue and sulfate was very little. This was different with that of the combustion of ARB in the absence of CuFe$_2$O$_4$ with the residues of some organic compounds and sulfate instead of nitrate. SEM/EDAX analysis also demonstrated much more N element on the surface of CuFe$_2$O$_4$ than S by mole ratio of N/S = 8.6/1 after combustion. To summarise, the main reaction process has been described in Table 3.

3.4. Reusability of CuFe$_2$O$_4$

Seven adsorption–combustion cycles were carried out to evaluate the reusability of magnetic CuFe$_2$O$_4$ powder as adsorbent/catalyst for the removal of ARB. Fig. 8 shows the removal of ARB during the seven cycles, from 50 ml solution of initial concentration 100 mg/l at pH 4.8. CuFe$_2$O$_4$ was washed after each combustion using a NaOH solution of pH 8–9 for the removal of nitrate and sulfate formed

Table 3
The main reaction processes of ARB and ARB/CuFe$_2$O$_4$ during combustion at different temperature

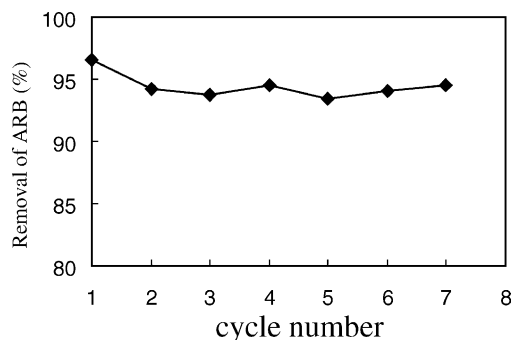| Temperature (°C)	Main groups reacted		Main products	
	ARB	ARB/CuFe$_2$O$_4$	ARB	ARB/CuFe$_2$O$_4$
150	–	–SO$_3^-$, –OH	–	SO$_2$
200–250	–	–SO$_3^-$, –OH, –N=N–	–	SO$_2$, R–NO$_2$
300	–SO$_3^-$, –N=N–	–C=C–, –NO$_2$	SO$_2$	CO$_2$, H$_2$O, NO$_3^-$
500	–SO$_3^-$, aromatic ring –C=C–, –OH, –N=N–	–	SO$_2$, CO$_2$, H$_2$O, SO$_4^{2-}$, R–C≡N, R–N=C=O, R–NO	–
600	–C=C–, R–C≡N, R–N=C=O, R–NO	–	CO$_2$, H$_2$O	–
Residue	–	–	PAHs, sulfate	Nitrate

Fig. 8. Reusability of $CuFe_2O_4$ for the removal of ARB during seven cycles, for 50 ml ARB solution of initial concentration 100 mg/l at pH 4.8.

in the oxidation reaction. The results demonstrated that the removal of ARB by $CuFe_2O_4$ adsorption from water only decreased slightly after the first cycle, and then it reached a stable state in the following cycles. Analyses of combustion products and FTIR study for the reaction process in the seventh cycle did not show evident change as compared to that of the first cycle. These experiments demonstrated that $CuFe_2O_4$ as adsorbent/catalyst could be used repeatedly over many cycles.

4. Conclusions

1. Magnetic $CuFe_2O_4$ powder was proven to possess excellent adsorptive properties towards azo-dye ARB at pH < 5.5. And it can be conveniently recovered by magnetic separation technology after adsorption.
2. $CuFe_2O_4$ powder has high catalytic activity for the combustion of adsorbed ARB. The oxidative combustion reaction could be carried out at relatively low temperature, and no organic product emitted to atmosphere or deposited on the $CuFe_2O_4$ surface after combustion.
3. Magnetic $CuFe_2O_4$ powder is an excellent adsorbent/catalyst for the removal of azo-dye ARB by adsorption–catalytic combustion and can be used repeatedly.

References

[1] H.H.W. Lee, G. Chen, P.L. Yue, Water Sci. Technol. 44 (5) (2001) 75.
[2] G. Bertanza, C. Collivignarelli, R. Pedrazzani, Water Sci. Technol. 44 (5) (2001) 109.
[3] S.H. Lee, D.I. Song, Y.W. Jeon, Environ. Technol. 22 (2001) 247.
[4] C. Catrinescu, C. Teodosiu, M. Macoveanu, J. Miehe-Brendle, R.L. Dred, Water Res. 37 (2003) 1154.
[5] S.J. Allen, Types of Adsorbent Materials—Use of Adsorbents for the Removal of Pollutants from Wastewaters, CRC, Boca Raton, FL, USA, 1996, p. 59.
[6] W.P. Kwan, B.M. Voelker, Environ. Sci. Technol. 37 (2003) 1150.
[7] L. Oliviero, J. Barbier Jr., D. Duprez, Appl. Catal. B 40 (2003) 163.
[8] E.A. Deliyanni, D.N. Bakoyannakis, A.I. Zouboulis, K.A. Matis, Chemosphere 50 (2003) 155.
[9] M. Baldi, V.S. Escribano, J.M.G. Amores, F. Milella, G. Busca, Appl. Catal. B 17 (1998) L175.
[10] B. Gu, J. Schmitt, Z. Chen, L. Liang, J.F. McCarthy, Environ. Sci. Technol. 28 (1994) 38.
[11] S.G.J. Heijman, A.M. Paassen, W.G.J. Meer, R. Hopman, Water Sci. Technol. 40 (9) (1999) 183.
[12] F. Herrera, A. Lopez, G. Mascolo, P. Albers, J. Kiwi, Appl. Catal. B 29 (2001) 147.
[13] A.F.M. van Velsen, G. van der Vos, Water Sci. Technol. 24 (10) (1991) 195.
[14] A.D. Ebner, J.A. Ritter, H.J. Ploehn, Sep. Sci. Technol. 34 (1999) 1277.
[15] R. Silverstein, T. Clayton, T. Morril, Spectrophotometric Identification of Organic Compounds, Wiley, New York, 1991, p. 106.
[16] G. Centi, Environmental Catalysis, Ital. Chem. Soc. Pub., Rome, 1995, p. 245.
[17] J. Bandara, J.A. Mielczarski, J. Kiwi, Langmuir 15 (1999) 7670.